Airborne Particulates Affect Corneal Homeostasis and Immunity

Mallika Somayajulu,[1] Sandamali Ekanayaka,[1] Sharon A. McClellan,[1] Denise Bessert,[1] Ahalya Pitchaikannu,[1] Kezhong Zhang,[2] and Linda D. Hazlett[1]

[1]Department of Ophthalmology, Visual and Anatomical Sciences and Center for Molecular Medicine and Genetics, Wayne State University School of Medicine, Detroit, Michigan, United States
[2]Center for Molecular Medicine and Genetics, Wayne State University School of Medicine, Detroit, Michigan, United States

Correspondence: Linda D. Hazlett, Department of Ophthalmology, Visual and Anatomical Sciences, Wayne State University School of Medicine, 540 E. Canfield Avenue, Detroit, MI 48201, USA; lhazlett@med.wayne.edu.

Received: January 13, 2020
Accepted: February 24, 2020
Published: April 17, 2020

Citation: Somayajulu M, Ekanayaka S, McClellan SA, et al. Airborne particulates affect corneal homeostasis and immunity. *Invest Ophthalmol Vis Sci.* 2020;61(4):23. https://doi.org/10.1167/iovs.61.4.23

Purpose. To determine the effects of airborne particulate matter (PM) <2.5 µm in vitro and on the normal and *Pseudomonas aeruginosa* (PA)-infected cornea.

Methods. An MTT viability assay tested the effects of $PM_{2.5}$ on mouse corneal epithelial cells (MCEC) and human corneal epithelial cells (HCET). MCEC were tested for reactive oxygen species using a 2′,7′-dichlorodihydrofluorescein assay; RT-PCR determined mRNA levels of inflammatory and oxidative stress markers in MCEC (HMGB1, toll-like receptor 2, IL-1β, CXCL2, GPX1, GPX2, GR1, superoxide dismutase 2, and heme oxygenase 1) and HCET (high mobility group box 1, CXCL2, and IL-1β). C57BL/6 mice also were infected and after 6 hours, the $PM_{2.5}$ was topically applied. Disease was graded by clinical score and evaluated by histology, plate count, myeloperoxidase assay, RT-PCR, ELISA, and Western blot.

Results. After $PM_{2.5}$ (25–200 µg/mL), 80% to 90% of MCEC and HCET were viable and PM exposure increased reactive oxygen species in MCEC and mRNA expression levels for inflammatory and oxidative stress markers in mouse and human cells. In vivo, the cornea of PA+$PM_{2.5}$ exposed mice exhibited earlier perforation over PA alone (confirmed histologically). In cornea, plate counts were increased after PA+$PM_{2.5}$, whereas myeloperoxidase activity was significantly increased after PA+$PM_{2.5}$ over other groups. The mRNA levels for several proinflammatory and oxidative stress markers were increased in the cornea in the PA+$PM_{2.5}$ over other groups; protein levels were elevated for high mobility group box 1, but not toll-like receptor 4 or glutathione reductase 1. Uninfected corneas treated with $PM_{2.5}$ did not differ from normal.

Conclusions. $PM_{2.5}$ triggers reactive oxygen species, upregulates mRNA levels of oxidative stress, inflammatory markers, and high mobility group box 1 protein, contributing to perforation in PA-infected corneas.

Keywords: particulates, mice, cornea, infection

Particulate matter (PM) is a general term for small solid and liquid particles in the atmosphere (a major air pollutant) that vary in size (e.g., $PM_{2.5}$–PM_{10}), composition, and origin.[1,2] There are many different sources of PM, including natural (e.g., forest fires[3]) and man made (e.g., diesel engines,[4] industry,[2] wood burning stoves,[5] and agricultural burning[6]) types. Exposure to particle pollution is detrimental to health[7] and has economic effects as well.[8] Previous studies have indicated that acute and chronic exposure to PM has increased the morbidity and mortality rate worldwide (e.g., the United States,[9] Europe,[10] and China[11]). Specifically, in cities with elevated air pollution levels compared with those without, the individual mortality risk is 26% greater.[1] $PM_{2.5}$ is a fine airborne PM with an aerodynamic diameter of <2.5 µm.[12] It is the major outdoor air pollutant in most urban areas worldwide (e.g., China,[13] the United States[14]) and a major pollutant in indoor air, especially in households that use biomass fuel for cooking and/or heating.[5,15] These particles are produced mainly from man-made sources and contain molecules composed of sulfates, nitrates, ammonia, carbon, lead, and organic compounds.[11] $PM_{2.5}$ is the major and most toxic air pollutant found in environments with heavy traffic and industrial activity and accounts for 5.5% of deaths and $5.1 billion in economic loss annually in urban cities such as Detroit, Michigan.[16] In addition, recent work has confirmed a correlation with modest $PM_{2.5}$ increase and mortality in the Medicare population.[17] Owing to its small size, $PM_{2.5}$ has an incremental capacity to penetrate different tissues via mucosal membranes (e.g., lung[18]). $PM_{2.5}$ is strongly associated with the pathogenesis of air pollution-associated diseases including cancer,[19–21] metabolic,[22–24] respiratory,[25–27] and cardiovascular[28,29] diseases, all of which are being investigated. For example, it has been reported that $PM_{2.5}$ exposure triggers a variety of maladaptive signaling pathways in the lung,[23,30–32] blood vessels,[33] liver,[22,23,34] and adipose tissues[35] that are associated with oxidative[29,32] and endoplasmic reticulum stress[23,35] and inflammatory responses.[31–33] A mucosal site

that has essentially been overlooked is the eye. Specifically, the ocular surface (e.g., cornea[1] and conjunctiva[1]) is continually exposed to air pollutants, including $PM_{2.5}$, which may lead to an adverse effect on the homeostasis of these tissues. However, little attention has been given to developing models to test the effects of $PM_{2.5}$ on ocular disease propensity. Epidemiologic and clinical data suggest that air pollution in which $PM_{2.5}$ is a major constituent can cause transient ocular allergies (redness,[1] foreign body sensation,[36] and itching[36]). It is also reported that in households that use biomass fuel for cooking and heating, there is a high risk of blindness (e.g., trachoma,[5] cataract[37]), especially among young children[5] and females.[37,38] In addition, limited in vitro studies using human corneal epithelial cells (HCET), have suggested, but did not provide mechanisms, by which $PM_{2.5}$ may promote autophagy,[39] damage mitochondrial function,[40] decrease cell viability,[41] and cause oxidative damage.[41] If bacteria are present, exposure of mucosal sites to PM may also enhance bacterial stress resistance mechanisms,[42,43] biofilm formation,[42,43] and enhance colonization.[42,43] In this regard, epidemiologic studies strongly suggest that it is biologically plausible to hypothesize that exposure to $PM_{2.5}$ is associated with some of the major blinding and painful eye conditions seen worldwide, including the development of corneal ulcers resulting from delayed wound healing after injury or infection.[5] Those studies further suggest that it is difficult to study clinical disease retrospectively and that experimental models are needed to test mechanistically the relationship between $PM_{2.5}$ exposure and ocular disease and infection. Other studies reveal a link between PM and increased outpatient visits for several ocular diseases, including allergic conjunctivitis[44] and emergency room visits for keratitis.[45] In this article, we report the effects of $PM_{2.5}$ exposure in mouse corneal epithelial cells (MCEC) in vitro, providing evidence that exposure: decreased cell viability and was concentration dependent, increased production of reactive oxygen species (ROS)/reactive nitrogen species (RNS), and inflammatory and oxidative stress associated molecules. A mouse model shows that $PM_{2.5}$ exposure together with *Pseudomonas aeruginosa* (PA) infection, leads to the upregulation of inflammatory and oxidative stress–associated molecules, a significant increase in infiltrating neutrophils, and an accelerated rate of corneal perforation compared with infected controls. We also show that decreased viability and increased levels of inflammatory molecules after $PM_{2.5}$ exposure of three-dimensional (3D) cultured HCET was concentration dependent.

Methods

$PM_{2.5}$ Samples

Real-world $PM_{2.5}$ particles were collected from June to August 2008 through Ohio's Air Pollution Exposure System for the Interrogation of Systemic Effects system. Samples were subjected to x-ray fluorescence spectroscopy to analyze composition. Concentrations of major $PM_{2.5}$ chemicals are shown in Table 1.[23] For the studies below, $PM_{2.5}$ was dissolved in sterile PBS for the concentrations indicated.

Tissue Culture

Cultured C57BL/6 MCEC were grown as described previously.[46] Immortalized HCET cells (10.014 pRSV-T, a gift from Dr Gabriel Sosne) were cultured in keratinocyte-serum free medium (Gibco, Grand Island, NY) with 5 ng/mL human recombinant epidermal growth factor, 0.05 mg/mL bovine pituitary extract, 0.005 mg/mL insulin, and 500 ng/mL hydrocortisone. HCET cells (1×10^4 cells) were plated on 96-well plates containing cultures Mimetix (Cambridge, MA) scaffold (PLLA, 4 micron fiber diameter, 50 micron thick; Catalog: AMS.TECL-002-1X). The cells were grown on the scaffolds to generate 3D cultures for 3 weeks per the manufacturer's instructions. Cells were then treated with $PM_{2.5}$ (0, 100, 200 and 500 µg/mL for 24 hours) for the MTT assay, and 100 µg/mL $PM_{2.5}$ for 24 hours and mRNA analyzed using RT-PCR.

Table 1. Composition of $PM_{2.5}$

Category	Chemical	Concentration, ng/m^3
Alkali metals	K	308.3 ± 75.1
	Na	375.0 ± 91.7
Alkaline earth metals	Mg	50.5 ± 16
	Ca	220.1 ± 54.1
	Sr	20.3 ± 3.5
Transition metals	Fe	385.0 ± 99.1
	Zn	115.9 ± 29.5
Poor metals	Al	53.0 ± 27.5
	Sn	55.0 ± 18.9
	Pb	19.9 ± 4.1
Lanthanoids	Sm	3.3 ± 1.8
Metals	Eu	1.5 ± 0.4
Nonmetals	S	9167.5 ± 913.1
	Si	833.4 ± 54.1

MTT Assay

The MTT 3-(4, 5-dimethylthiazol-2-yl)-2,5-diphenyltetrazolium bromide (ThermoFisher Scientific, Grand Island, NY) assay was used to evaluate the effects of PM on cell viability. The assay was performed according to manufacturer's protocol. Briefly, 15,000 MCEC were cultured in 96-well plates overnight and exposed to various concentrations of $PM_{2.5}$ (0, 25, 50, 100, 200, 500, 800, and 1200 µg/mL) for 24 hours. At the end of the treatment, 5 mg/mL of MTT reagent was added to each well. The plate was then incubated at 37°C for 4 hours and the media removed. Dimethyl sulfoxide was added (50 µL/well) to dissolve the metabolic product formazan and the plate was placed on a shaker at 150 rpm for 5 minutes. Optical density was read at 540 nm using a SpectraMax M5 microplate reader (Molecular Devices, Sunnyvale, CA). HCET grown in 3D cultures were exposed to 100, 200, and 500 µg/mL $PM_{2.5}$ for 24 hours before the MTT assay.

Measurement of ROS/RNS Levels

ROS/RNS levels in MCEC were measured using an OxiSelect in vitro ROS/RNS Assay Kit (Cell Biolabs, Inc., San Diego, CA) per the manufacturer's instructions. The assay uses a proprietary quenched fluorogenic probe, dichlorodihydrofluorescin DiOxyQ (DCFH-DiOxyQ), which is a specific ROS/RNS probe that is based on similar chemistry to the popular 2′,7′-dichlorodihydrofluorescein diacetate. The DCFH-DiOxyQ probe is first primed with a quench removal

reagent, and subsequently stabilized in the highly reactive DCFH form. In this reactive state, ROS and RNS species can react with DCFH, which is rapidly oxidized to the highly fluorescent 2′,7′-dichlorodihydrofluorescein (DCF). The fluorescence intensity of DCF is proportional to total ROS/RNS levels. Briefly, $PM_{2.5}$-treated (0, 25, 50, or 100 µg/mL) MCEC were homogenized in 500 µL of cold PBS and centrifuged at 10,000*g* for 5 minutes. A 50-µL aliquot of each supernatant was added to a 96-well black microtiter plate in duplicate and incubated with 50 µL of catalyst for 5 minutes, followed by incubation with 100 µL of DCFH for 30 minutes. DCF fluorescence was measured at 480 nm (excitation) and 530 nm (emission).Total ROS/RNS concentration in MCEC homogenates was determined by generating a DCF standard curve. Fluorescence was measured using a SpectraMax M5 spectrophotometer.

Mice

Eight-week-old female C57BL/6 mice were purchased from the Jackson Laboratory (Bar Harbor, ME) and housed in accordance with the National Institutes of Health guidelines. They were humanely treated and in compliance with both the ARVO Statement for the Use of Animals in Ophthalmic and Vision Research and the Institutional Animal Care and Use Committee of Wayne State University (IACUC 18-08-0772).

Bacterial Culture

A previously published protocol was followed to culture bacteria.[47] Briefly, PA cytotoxic strain, 19660 (American Type Culture Collection Manassas, VA) was grown in peptone tryptic soy broth medium in a rotary shaker water bath at 37°C and 150 rpm for 18 hours to an optical density (measured at 540 nm) between 1.3 and 1.8. Bacterial cultures were centrifuged at 5500g for 10 minutes; pellets were washed once with sterile saline, recentrifuged, resuspended, and diluted in sterile saline.

Bacterial Infection and $PM_{2.5}$ Exposure

The C57BL/6 mice were anesthetized using anhydrous ethyl ether mice and placed beneath a stereoscopic microscope at ×40 magnification. The left cornea was scarified with three 1-mm incisions using a sterile $25^{5/8}$-gauge needle. The wounded corneal surface was then topically treated with 5 µL containing 1×10^6 colony forming units (CFU)/µL PA 19660.[47,48] Six hours later and then twice at 1 day post infection (p.i.), one group was exposed (topical application onto cornea) to $PM_{2.5}$ (2 µg/5 µL dose; from a concentration of 400 µg/mL), and the other infected group received PBS similarly. Uninfected, wounded mouse corneas were similarly exposed to $PM_{2.5}$ only. Uninfected normal controls were not wounded or treated with PBS.

Ocular Response to Bacterial Infection and $PM_{2.5}$ Exposure

An established corneal disease grading scale was used to assign a clinical score value to each infected eye. [49] Disease was graded as follows: 0, clear/slight opacity, partially or fully covering the pupil; +1, slight opacity, covering the anterior segment; +2, dense opacity, partially or fully covering the pupil; +3, dense opacity, covering the anterior segment; and +4, corneal perforation. Each mouse was scored in masked fashion at 1 and 2 days p.i. for statistical comparison and photographed (2 days p.i.) with a slit lamp to illustrate disease.

Histopathology

Infected eyes ($n = 3$/treatment/time) were enucleated from uninfected and infected mice exposed to $PM_{2.5}$ or PBS at 2 days p.i., immersed in PBS, rinsed, and fixed in 1% osmium tetroxide (Electron Microscopy Sciences, Hatfield, PA), 2.5% glutaraldehyde (Electron Microscopy Sciences) and 0.2 M Sorenson's phosphate buffer (pH 7.4) 1:1:1 at 4°C for 3 hours. Eyes were rinsed with 0.1 M phosphate buffer, dehydrated in ethanol and propylene oxide (Sigma-Aldrich, St. Louis, MO), infiltrated and embedded in Eponaraldite (Electron Microscopy Sciences). Sections (1.5 µm) were cut, stained with Toluidine blue and photographed (Leica DM4000B, Leica Microsystems, Inc., Buffalo Grove, IL), as described previously.[50]

Quantification of Viable Bacteria

Corneas from each of the three groups (PA+$PM_{2.5}$ or PBS and $PM_{2.5}$ only) were removed at 2 days p.i. Each cornea was homogenized in 1 mL of sterile saline containing 0.25% BSA and 100 µL was serially diluted 1:10 in sterile saline containing 0.25% BSA. Selected dilutions were then plated in triplicate on Pseudomonas isolation agar plates (Becton-Dickinson, Franklin Lakes, NJ) and incubated overnight at 37°C. Bacterial colonies were manually counted and reported as $\log_{10}$ CFU/plate +SEM.[50]

Myeloperoxidase (MPO) Assay

This assay was used to enumerate neutrophils in the cornea of the three groups (described in viable plate count elsewhere in this article) of mice. A previously published protocol was used for the assay.[50] Briefly, individual corneas were removed at 2 days p.i. and homogenized in 1 mL of of 50 mM phosphate buffer (pH 6.0) containing 0.5% hexadecyltrimethyl-ammonium (Sigma-Aldrich). Samples were freeze-thawed four times, centrifuged, and 100 µL of the supernatant added to 2.9 mL of 50 mM phosphate buffer containing o-dianisidine dihydrochloride (16.7 mg/mL; Sigma-Aldrich) and hydrogen peroxide (0.0005%). The change in absorbency was monitored at 460 nm for 4 minutes at 30-second intervals. The slope of the line was determined for each sample and used to calculate units of MPO/cornea. One unit of MPO activity equals approximately 2×10^5 neutrophils.[50]

RT-PCR

For in vitro assays, MCEC (50,000 cells/well) were grown in 24-well plates and exposed to 0, 25, or 100 µg/mL $PM_{2.5}$ for 24 hours at 37°C. For 3D HCET cultures, cells were grown in 96-well plates for 3 weeks and exposed to 100 µg/mL $PM_{2.5}$ for 24 hours at 37°C. For in vivo experiments,

Investigative Ophthalmology & Visual Science

Table 2. Nucleotide Sequence of the Specific Primers Used for PCR Amplification (Human)

Gene	Nucleotide Sequence	Primer	GenBank
GAPDH	5′-GGA GCG AGA TCC CTC CAA AAT-3′	F	NM_002046.7
	5′- GGC TGT TGT CAT ACT TCT CAT GG-3′	R	
HMGB1	5′- TGG CCA AGG AAT CCA GCA GTT-3′	F	NM_001313893.1
	5′- CTC CTC CCG ACA AGT TTG CAC-3′	R	
IL-1β	5′- TTC GAG GCA CAA GGC ACA AC-3′	F	NM_000576.2
	5′- TTC ACT GGC GAG CTC AGG TA-3′	R	
CXCL2	5′-AGC TTG TCT CAA CCC CGC ATC-3′	F	NM_002089.4
	5′-TTA GGC GCA ATC CAG GTG GC-3′	R	

F, forward; R, reverse.

Table 3. Nucleotide Sequence of the Specific Primers Used for PCR Amplification (Mouse)

Gene	Nucleotide Sequence	Primer	GenBank
β-actin	5′- GAT TAC TGC TCT GGC TCC TAG C-3′	F	NM_007393.3
	5′- GAC TCA TCG TAC TCC TGC TTG C-3′	R	
Hmgb1	5′- TGG CAA AGG CTG ACA AGG CTC-3′	F	NM_010439.3
	5′- GGA TGC TCG CCT TTG ATT TTG G-3′	R	
Tlr2	5′- CTC CTG AAG CTG TTG CGT TAC -3′	F	NM_011905.3
	5′- TAC TTT ACC CAG CTC GCT CAC TAC-3′	R	
Tlr4	5′- CCT GAC ACC AGG AAG CTT GAA-3′	F	NM_021297.2
	5′- TCT GAT CCA TGC ATT GGT AGG T-3′	R	
Il-1β	5′-TGT CCT CAT CCT GGA AGG TCC ACG-3′	F	NM_008361.3
	5′-TGT CCT CAT CCT GGA AGG TCC ACG-3′	R	
Cxcl2 (*Mip2*)	5′-TGT CAA TGC CTG AAG ACC CTG CC-3′	F	NM_009140.2
	5′-AAC TTT TTG ACC GCC CTT GAG AGT GG -3′	R	
Gpx1	5′-CTC ACC CGC TCT TTA CCTTCC T-3′	F	NM_008160.6
	5′-ACA CCG GAG ACC AAA TGA TGT ACT-3′	R	
Gpx2	5′-GTG GCG TCA CTC TGA GGA ACA-3′	F	NM_030667
	5′-CAG TTC TCC TGA TGT CCG AAC TG-3′	R	
Gr1	5′-CCA CGG CTA TGC AAC ATT CG-3′	F	NM_010344.4
	5′-GAT CTG GCT CTC GTG AGG AA-3′	R	
Sod2	5′-GCG GTC GTGTAA ACC TCA AT-3′	F	NM_013671
	5′-CCA GAG CCT CGT GGT ACT TC-3′	R	
Ho1	5′-CAC GCA TAT ACC CGC TAC CT-3′	F	NM_010442
	5′-CCA GAG TGT TCA TTC GAG C-3′	R	

F, forward; R, reverse.

normal (uninfected) and/or exposed to $PM_{2.5}$ (2 µg/5 µL dose) and infected (PA 19660) corneas exposed to PBS or $PM_{2.5}$ were harvested at 2 days p.i. from C57BL/6 mice. For both in vitro and in vivo assays, total RNA was isolated (RNA STAT-60; Tel-Test, Friendswood, TX) per the manufacturer's instructions, as reported previously.[50] One microgram of each RNA sample was reverse transcribed using Moloney-murine leukemia virus reverse transcriptase (Invitrogen, Carlsbad, CA) to produce a cDNA template PCR. The cDNA products were diluted 1:20 with DEPC-treated water and a 2-µL aliquot of diluted cDNA was used for the RT-PCR reaction. SYBR green/fluorescein PCR master mix (Bio-Rad Laboratories, Richmond, CA) and primer concentrations of 10 µM were used in a total 10 µL volume. After a preprogrammed hot start cycle (3 minutes at 95°C), the parameters used for PCR amplification were: 15 seconds at 95°C and 60 seconds at 60°C with the cycles repeated 45 times. Levels of high mobility group box 1 (HMGB1), toll-like receptor (TLR) 2, TLR4, IL-1β, chemokine (C-X-C) ligand 2 (CXCL2), glutathione peroxidase (GPX) 1 , GPX2, glutathione reductase 1 (GR1), superoxide dismutase 2 (SOD2), and heme oxygenase 1 (HO1) were tested by real-time RT-PCR (CFX Connect real-time PCR detection system; Bio-Rad Laboratories). The fold differences in gene expression were calculated relative to housekeeping genes β-actin (mouse) and GAPDH (human) and expressed as the relative mRNA concentration ± SEM. Primer pair sequences used are shown in Tables 2 and 3. Data are shown as mean ± SEM.

ELISA and Western Blotting

Corneas were harvested (2 days p.i.) from normal mice, mice that were uninfected and exposed to $PM_{2.5}$, and PA-infected mouse corneas exposed to PBS or $PM_{2.5}$. Pooled samples were suspended in PBS containing protease and phosphatase inhibitors (ThermoFisher, Rockford, IL), sonicated, and centrifuged at 12,000*g* for 20 minutes. Total protein was determined (Micro BCA protein kit; ThermoFisher). TLR4 was detected by Western blot. A previously published protocol was used for Western blot.[51] Briefly, samples (30 µg) were run on sodium dodecyl sulfate polyacrylamide gel electrophoresis in Tris-glycine-SDS buffer and electro-blotted

Investigative Ophthalmology & Visual Science

onto nitrocellulose membranes. After blocking for 1 hour in 5% Tris buffer saline containing 0.05% Tween 20 (TBST) and 5% nonfat milk (MTBST), membranes were probed with primary antibodies: rabbit anti-mouse TLR4 (1:1000; Abcam Cambridge, MA) in 3% BSA TBST overnight at 4°C. After 3 washes with TBST, membranes were incubated with horseradish peroxidase-conjugated anti-rabbit secondary antibody (1:2000; Cell Signaling Technology, Danvers, MA) diluted in 5% MTBST at room temperature for 2 hours. Bands were developed with Supersignal West Femto Chemiluminescent Substrate (ThermoFisher), visualized using an iBright Imaging System (ThermoFisher), normalized to β-actin and intensity quantified using AlphaView software.

Individual corneas from normal, uninfected mice, uninfected mice exposed to $PM_{2.5}$, and PA-infected mice exposed to PBS or $PM_{2.5}$ were harvested in 500 µL of PBS containing 0.1% Tween 20 and protease inhibitors. HMGB1 (Chondrex, Inc., Redmond, WA) and GR1 (MyBiosource, San Diego, CA) were detected by ELISA per the manufacturers' protocol.

Statistical Analysis

A Student's *t*-test was used to determine the significance of RT-PCR (3D HCET), ELISA, and Western blot data. An in vivo comparison of clinical scores between two groups at each time was tested by the Mann-Whitney *U* test. A one-way ANOVA followed by the Bonferroni's multiple comparison test was used for MTT (MCEC, 3D HCET), DCF, plate counts, MPO, and RT-PCR (MCEC, cornea). Data were considered significant at a P value of <0.05. All experiments were repeated at least once to ensure reproducibility and data are shown as mean ± SEM.

Results

$PM_{2.5}$ Exposure Affects Cell Viability and Increases ROS/ RNS Levels

In vitro, MCEC cells exposed to $PM_{2.5}$ for 24 hours showed a concentration-dependent decrease ($P < 0.001$) in live cells (Fig. 1A). At concentrations of 25 to 200 µg/mL, 80% to 90% of the cells were viable compared with controls. Even at 1200 µg/mL, the highest concentration tested, 60% remained viable. Figure 1B shows a concentration-dependent significant ($P < 0.05$, $P < 0.01$ and $P < 0.001$, respectively) increase in detectable ROS/RNS levels in MCEC exposed for 24 hours to lower concentrations of $PM_{2.5}$ (0, 25, 50, and 100 µg/mL) compared with controls (media exposed).

$PM_{2.5}$ Increases Levels of Proinflammatory and Oxidative Stress Markers In Vitro

RT-PCR tested if $PM_{2.5}$ (25 and 100 µg/mL for 24 hours) enhanced proinflammatory and oxidative stress molecules in MCEC (Figs. 2A–I). Except for CXCL2 and HO1 (Figs. 2D,E), mRNA levels of HMGB1 ($P < 0.05$), TLR2 ($P < 0.05$), IL-1β ($P < 0.05$), GR1 ($P < 0.05$), GPX1 ($P < 0.001$), GPX2 ($P < 0.001$), and SOD2 ($P < 0.05$) were significantly increased at 25 µg/mL $PM_{2.5}$. All molecules (Figs. 2A–I) also were significantly increased at 100 µg/mL $PM_{2.5}$ ($P < 0.001$ except GPX2, $P < 0.01$) when compared with media controls.

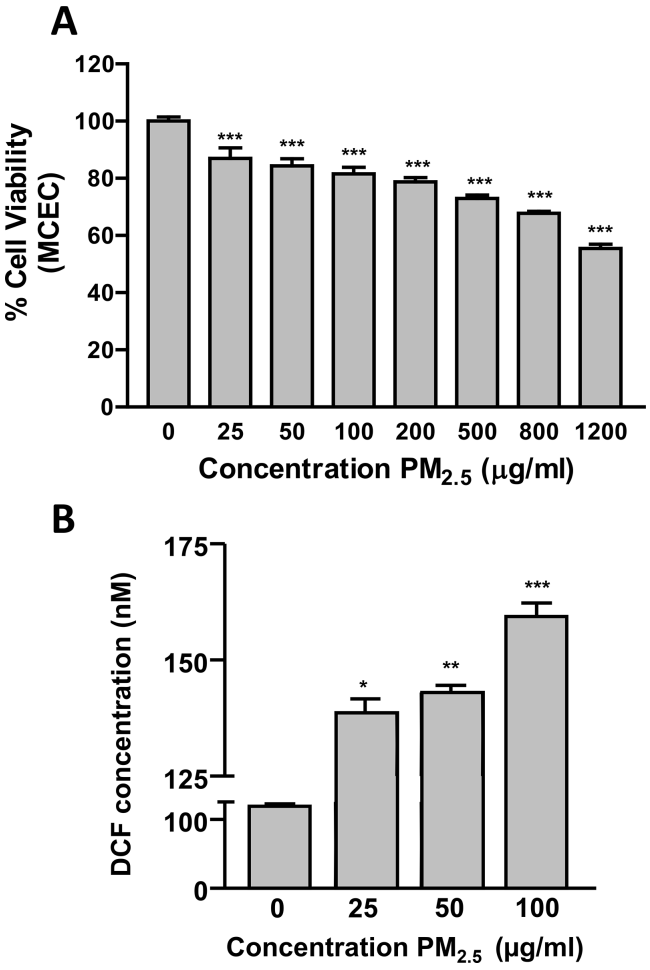

Figure 1. Effects of $PM_{2.5}$ exposure on cell viability and ROS production in MCEC in vitro. (**A**) Cells were exposed to 0, 25, 50,100, 200, 500, 800, and 1200 µg/mL concentrations of $PM_{2.5}$ for 24 hours. There is a significant decrease in cell viability when $PM_{2.5}$ concentration is increased. (**B**) Effects of $PM_{2.5}$ exposure on ROS formation in MCEC. Total ROS production in MCEC was measured 24 hours after treatment with 0, 25, 50, and 100 µg/mL $PM_{2.5}$ using DCF. Increasing the concentration of $PM_{2.5}$ significantly increased ROS levels. Data were analyzed using one-way ANOVA followed by Bonferroni's multiple comparison test and expressed as DCF concentration (normalized to control) ± SEM of triplicate experiments.*$P < 0.05$, **$P < 0.01$, ***$P < 0.001$.

$PM_{2.5}$ Exposure In Vivo Affects Ocular Response After PA Infection

Figure 3A–F shows data after topical $PM_{2.5}$ (2 µg/5 µL dose) exposure of PA-infected corneas. Clinical disease scores (Fig. 3A) showed significantly enhanced disease in both PBS and/or $PM_{2.5}$ exposed infected eyes when compared with $PM_{2.5}$ exposed uninfected eyes at 1 day p.i. ($P < 0.001$ for each). At 2 days p.i., significant differences were seen between the two infected groups ($P < 0.001$) in that the infected eyes exposed to $PM_{2.5}$ had more severe disease, including early perforation and reflected in worsened clinical scores. Photos taken with a slit lamp of typical eyes from infected, PBS (Fig. 3C), or $PM_{2.5}$ exposed (Fig. 3D) mice at 2 days p.i. showed central corneal thinning only in the infected $PM_{2.5}$ exposed eye. Exposure to the particulate

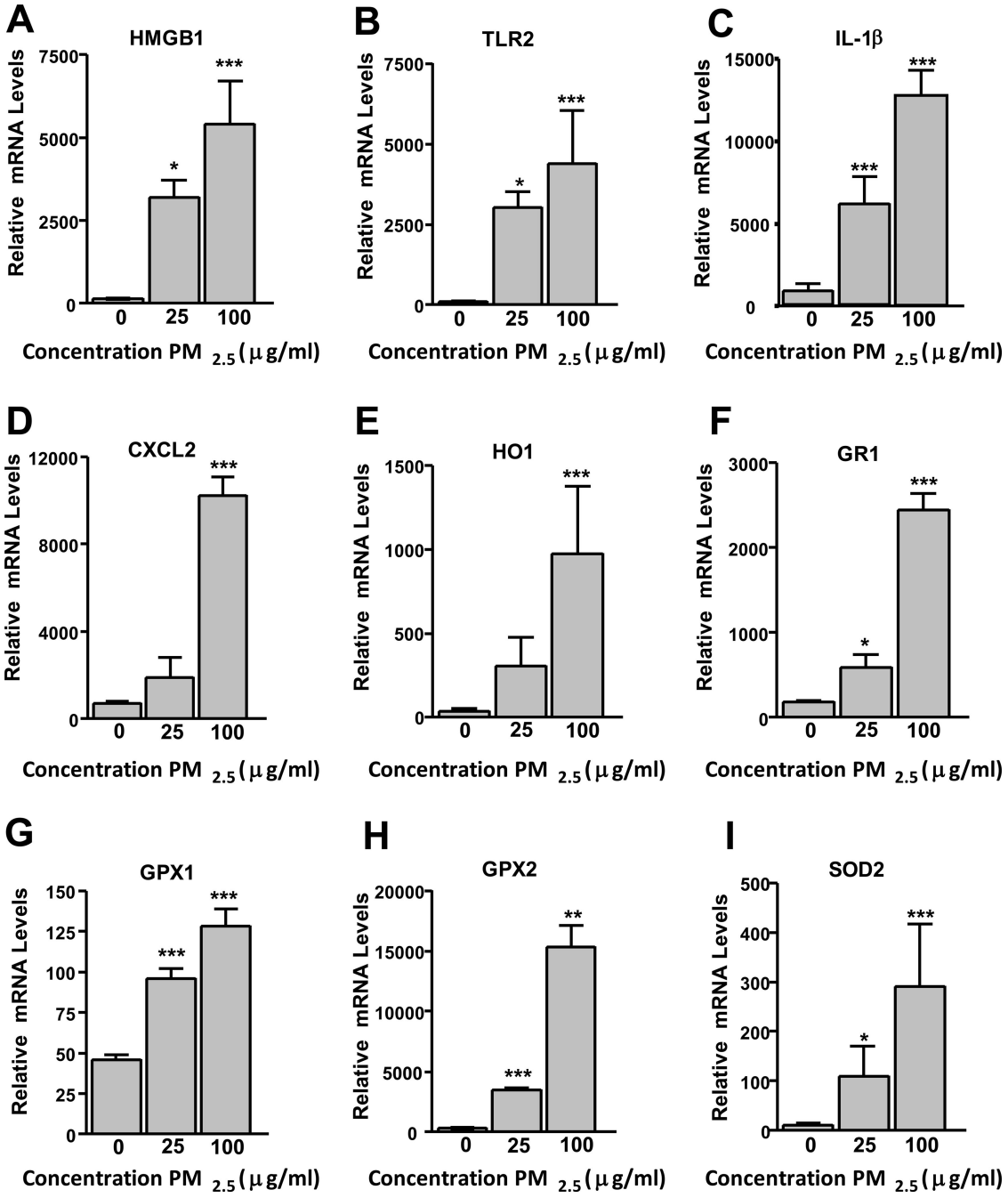

Figure 2. Effects of $PM_{2.5}$ exposure on proinflammatory and oxidative stress molecules in MCEC. RT-PCR shows significantly increased mRNA expression only for HMGB1 (**A**), TLR2 (**B**), IL-1β (**C**), GR1 (**F**), GPX1 (**G**), GPX2 (**H**), and SOD2 (**I**) at 25 μg/mL $PM_{2.5}$. All molecules (**A–I**) were significantly increased at 100 μg/mL $PM_{2.5}$ when compared with media controls. Data were analyzed using one-way ANOVA followed by Bonferroni's multiple comparison test and expressed as the mean ± SEM of triplicate experiments. *$P < 0.05$, **$P < 0.01$, ***$P < 0.001$.

alone did not cause observable corneal disease (Fig. 3B). A viable plate count (Fig. 3E) showed no significant difference in CFU per plate (actual counts) between infected groups, but there were more bacteria in the $PM_{2.5}$ exposed infected eye. An MPO assay (Fig. 3F) detected more PMN in the infected $PM_{2.5}$ versus PBS ($P < 0.001$) exposed corneas at 2 days p.i. Significant differences also were seen after infection and either PBS ($P < 0.001$) or $PM_{2.5}$ ($P < 0.001$) versus no infection and $PM_{2.5}$ exposure.

Histopathology

Figures 4A–F illustrates histopathology at 2 days p.i. in eyes exposed to $PM_{2.5}$ (Figs. 4A, D), to PBS+PA (Figs. 4B, E), and to $PM_{2.5}$+PA (Figs. 4C, F). Unexposed eyes (data not shown) were similar to the particulate exposed eyes (Figs. 4A, D). Eyes seemed to be normal; no infiltrate or particulate was visible in the cornea or the anterior chamber (Figs. 4A, D). In contrast, the cornea of PA exposed eyes showed modest

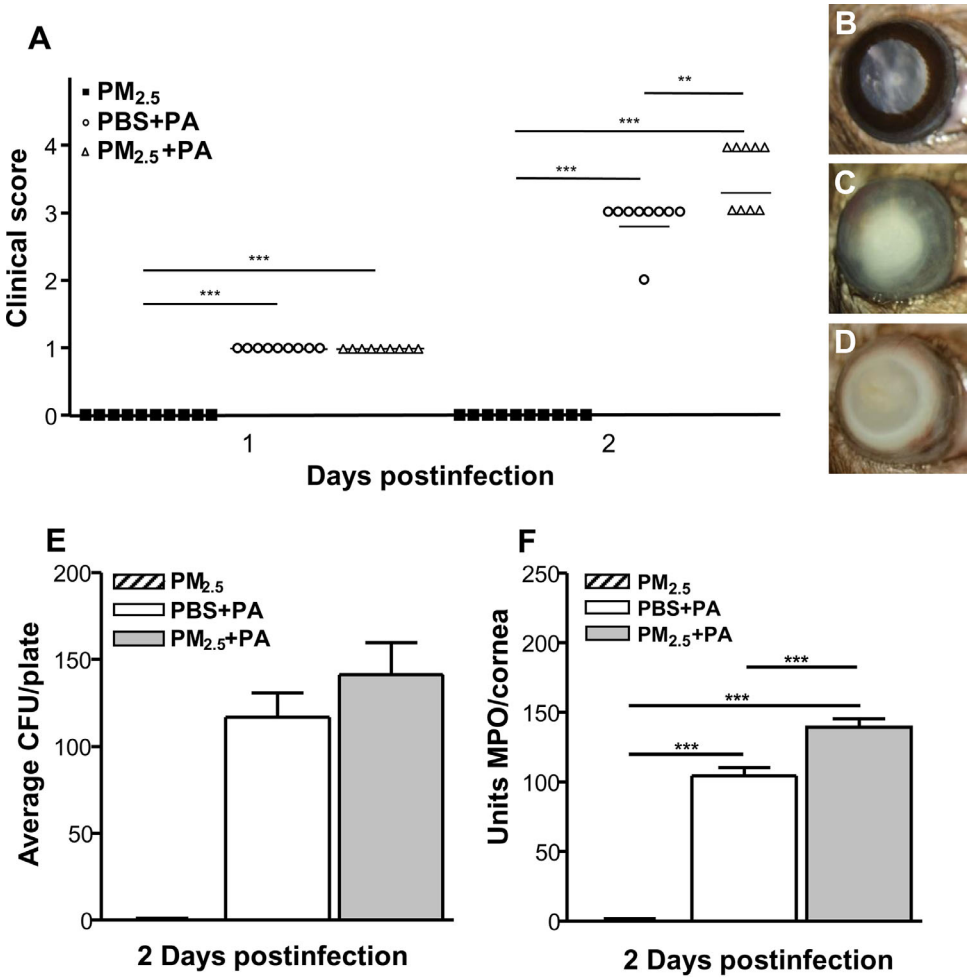

Figure 3

Figure 3. Disease response: Clinical scores, slit lamp photos, plate counts, and MPO assay after PA infection and $PM_{2.5}$. Topical exposure with $PM_{2.5}$ began at 6 hours p.i. Clinical scores, recorded 1 and 2 days p.i., showed significantly increased disease at 1 day p.i. comparing either infected eye with particulate alone. At 2 days p.i., disease was significantly worse in $PM_{2.5}$+PA versus PBS+PA or $PM_{2.5}$ alone (**A**). *Horizontal lines* indicate median values. Photographs taken with a slit lamp of eyes of C57BL/6 mice at 2 days p.i. from $PM_{2.5}$ no PA (**B**), PBS+PA (**C**), and $PM_{2.5}$+PA (**D**) illustrate the disease response. Viable bacterial plate count (**E**) and levels of MPO (**F**) were increased at 2 days p.i. (significant only for MPO) in the PBS+PA and $PM_{2.5}$+PA groups. Data was tested by the Mann-Whitney *U* test (clinical scores) and by one-way ANOVA followed by Bonferroni's multiple comparison test for plate count and MPO and expressed as the mean ± SEM ($n = 5$ per group at a time). $^{**}P < 0.01$, $^{***}P < 0.001$.

swelling and a cellular infiltrate in the cornea and anterior chamber (Figs. 4B, E). In PA and particulate exposed eyes corneal thinning, a heavy cellular infiltrate, particularly in the peripheral cornea, extensive stromal swelling, and destruction was observed (Figs. 4C, F). The inset in Figure 4C shows a higher magnification of the epithelium containing particulates and an inflammatory cell in close association with the epithelial surface.

$PM_{2.5}$ Effects on Proinflammatory and Oxidative Stress Molecules in the Mouse Cornea

The mRNA levels were also measured after in vivo exposure of infected mice to $PM_{2.5}$ (Figs. 5A–I). When comparing infected PBS versus $PM_{2.5}$ exposed eyes, significantly elevated mRNA levels were seen for TLR2 ($P < 0.001$), TLR4 ($P < 0.001$), IL-1β ($P < 0.05$), CXCL2 ($P < 0.01$), HO1 ($P < 0.001$), GR1 ($P < 0.01$), and SOD2 ($P < 0.05$). After $PM_{2.5}$ exposure, HMGB1 levels were decreased ($P < 0.01$) compared with normal (uninfected, unexposed) levels, but there was no difference between the two infected groups. In contrast, when comparing $PM_{2.5}$ exposed with normal corneas, TLR4 levels were increased ($P < 0.001$). No differences were seen between normal (uninfected, unexposed) and $PM_{2.5}$ exposed corneas when comparing all of the other molecules tested.

Protein Levels

ELISA was used to determine the relative corneal protein expression of HMGB1 (Fig. 6A) and GR1 (Fig. 6D), and

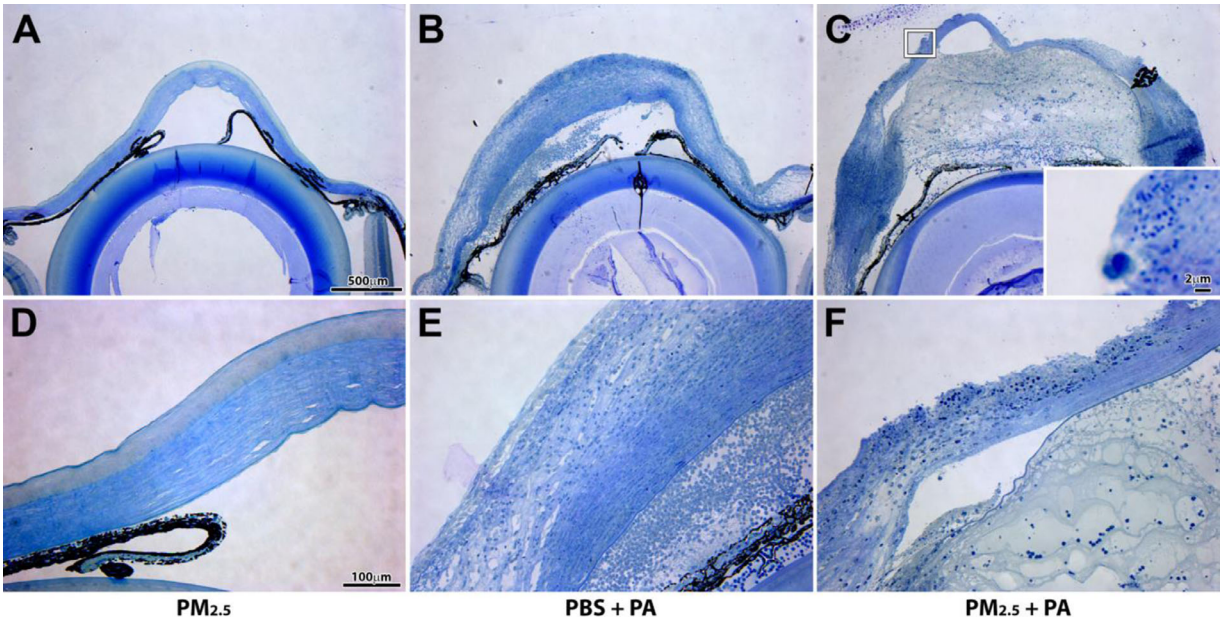

Figure 4. Histopathology (**A–F**). Extreme corneal thinning and a heavy cellular infiltrate in the stroma and anterior chamber was most pronounced in the eyes of $PM_{2.5}$+PA versus PBS+PA eyes at 2 days p.i. (**B**, **E** compared with **C**, **F**). The inset shows particulates in the corneal epithelium and an inflammatory cell (inset, **C**). The eyes exposed only to $PM_{2.5}$ (**A**, **D**) showed no infiltrated cells into cornea and anterior chamber, and less edema, at 2 days p.i. ($n = 3$ per time). Magnification: **A–C**, *scale bar*: 500 µm; **D–F** = 100 µm; inset = 2 µm.

Western blot analysis was used to determine TLR4 expression (Figs. 6B, C). At 2 days p.i., HMGB1 protein levels were increased after infection in $PM_{2.5}$ and PBS exposed groups. However, HMGB1 protein levels were significantly higher ($P < 0.05$) in $PM_{2.5}$+PA over PBS+PA (Fig. 6A) corneas. After infection, TLR4 protein levels were elevated but did not differ between the two groups (Figs. 6B, C). At 2 days p.i. GR1 protein levels remained unchanged in all four groups (Fig. 6D). HO1 levels also were tested using ELISA, but were undetectable (data not shown) at 2 days p.i.

Effects of $PM_{2.5}$ on The Viability of HCETs

To test the applicability of the in vivo mouse data to human corneal epithelium, we used 3D HCET cultures to test the effects of $PM_{2.5}$ exposure (0, 100, 200, and 500 µg/mL) for 24 hours. Compared with media controls, cells remained 80% viable at the lower concentrations ($P < 0.001$); at the highest concentration tested, approximately 60% remained viable ($P < 0.001$) (Fig. 7).

Effects of $PM_{2.5}$ on Proinflammatory Modulators in HCET Grown in 3D Cultures

The 3D HCET cultures were exposed to 100 µg/mL of $PM_{2.5}$ for 24 hours and mRNA levels of HMGB1, IL-1β, and CXCL2 were measured. The mRNA levels were significantly upregulated for all ($P < 0.01$, $P < 0.05$, $P < 0.05$, respectively) (Figs. 8A–C).

Discussion

PM exposure has been linked to multiple systemic diseases, including pulmonary,[33] cardiovascular,[28,29] and cerebrovascular,[52] where numerous studies are ongoing. Less well-studied, exposure also has been linked to eye itching,[53,54] tears, burning,[53,54] conjunctival congestion,[53,54] augmented mucus secretion,[53,54] conjunctival keratoconus,[53,54] swelling of the eyelids,[53,54] and conjunctival edema.[53,54] In this regard, epidemiologic evidence suggests that airborne and household pollutants exacerbate blinding and painful eye conditions observed worldwide.[5] These studies also suggested the need for laboratory studies to test this hypothesis.[5] Most important, more recent work reported in a clinical study in a population exposed to high levels of PM_{10} (PM < 10 µm,[45] which includes $PM_{2.5}$) revealed a link between PM and increased outpatient visits for several ocular diseases, including keratitis. Furthermore, it has been suggested that, at various air quality tested sites, the absorbance of $PM_{2.5}$ captures nearly all measurable particle absorbance,[55] yet many studies focus only on PM_{10} effects.[45] Additionally, $PM_{2.5}$ is the major and most toxic air pollutant found in urban environments.[16] Thus, we tested exposure to $PM_{2.5}$ on MCEC and HCETs in vitro. We also modified an in vivo mouse model to test the effects of the particulate on PA-induced keratitis. First, we evaluated the effects of $PM_{2.5}$ in vitro using MCEC. The data showed that increasing concentrations of $PM_{2.5}$ led to increased loss in cell viability, as well as increased ROS production (Fig 1A, B). Similar results have been observed in primary cultures of HCETs, exposed to indoor dust,[56,57] as well as RAW264.7 (macrophages) in vitro,[58,59] where oxidative stress was found to play a role in cytotoxicity. Next, using MCEC, we examined the effects of $PM_{2.5}$ on molecules important in the innate immune and/or oxidative stress response. We observed that $PM_{2.5}$ exposure

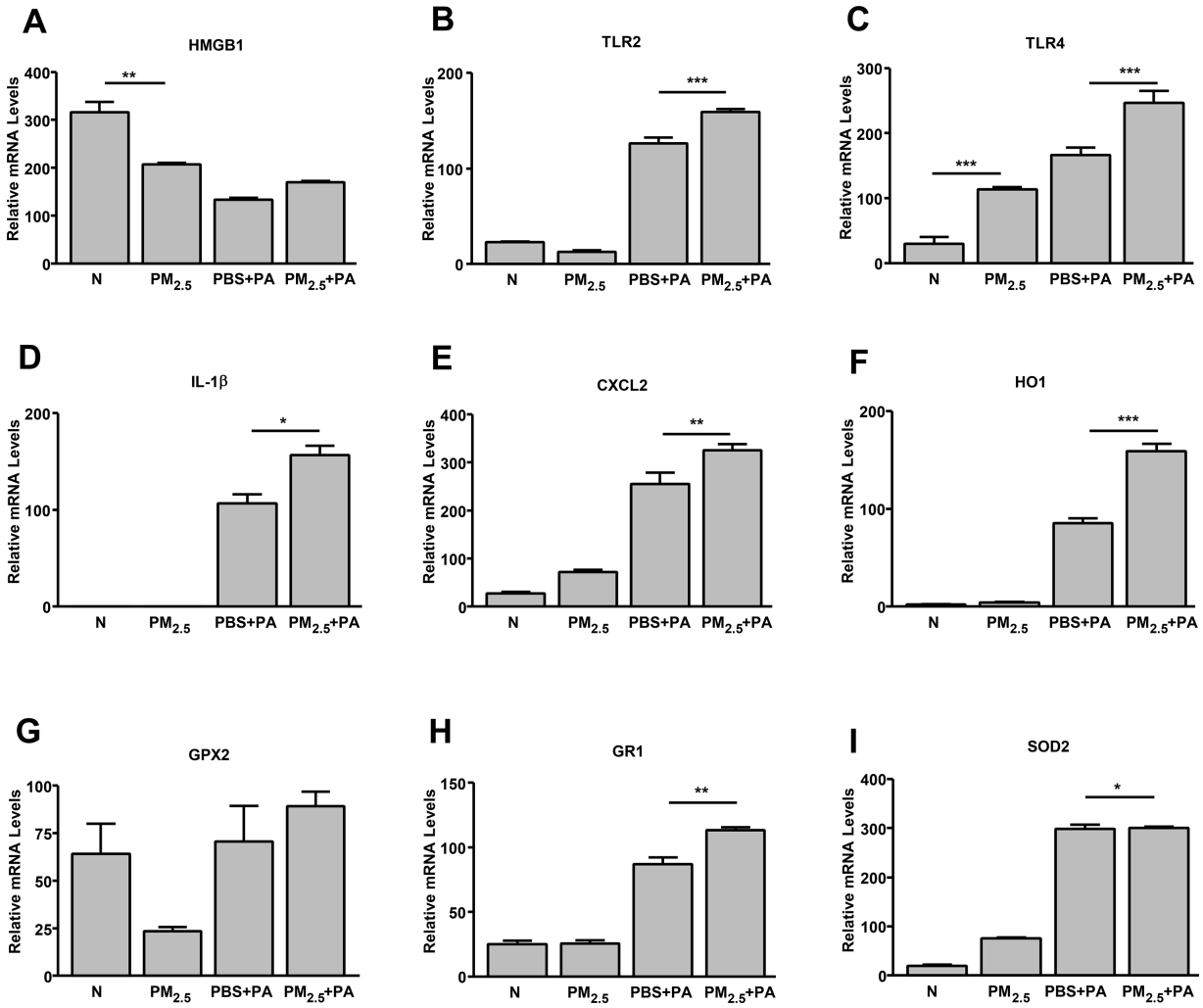

Figure 5. Effects of $PM_{2.5}$ and PA infection on inflammation and oxidative stress markers in vivo. RT-PCR showed significantly reduced mRNA expression for HMGB1 in PA infected versus uninfected groups (**A**). Increased mRNA levels for TLR2 (**B**), TLR4 (**C**), IL-1β (**D**), CXCL2 (**E**), HO1 (**F**), GPX2 (**G**), GR1 (**H**), and SOD2 (**I**) were observed in PA infected groups. In addition, $PM_{2.5}$ elevated mRNA levels of TLR4 (**C**) in uninfected eyes. Data were analyzed using one-way ANOVA followed by Bonferroni's multiple comparison test and expressed as the mean ± SEM. ($n = 5$ per group at a time). *$P < 0.05$, **$P < 0.01$, ***$P < 0.001$.

increased mRNA levels of HMGB1, TLR2, IL-1β, CXCL2, HO1, GR1, GPX1, GPX2, and SOD2. These data in corneal epithelial cells are consistent with a study in mouse lung (alveolar) macrophages, providing evidence that $PM_{2.5}$ induced increases in mRNA levels of molecules also associated with innate immunity, such as TLR4, IL-1β and TNF-α.[60] The data also are consistent with studies using human airway epithelial cells, which showed that HMGB1 mRNA levels were elevated[61] and other work that provided evidence that SOD and GPX1 levels in plasma[62] were significantly increased after particulate exposure.

To further determine the effects of $PM_{2.5}$ on keratitis, we also developed/modified an in vivo mouse model that uses C57BL/6 mice for PA studies.[63,64] After 6 hours p.i., $PM_{2.5}$ (2 µg/5 µL dose; made from a concentration of 400 µg/mL) was topically applied. This dose was selected based on work by Wang and colleagues,[65] who tested intratracheal installation of low (0.2 mg), medium (0.8 mg), and high (3.2 mg) $PM_{2.5}$ per animal. We also considered both annual (chronic) $PM_{2.5}$ levels in countries such as China[66] and India,[67] which range from 100 to 200 µg/m^3 and that in China, hourly $PM_{2.5}$ acute exposure levels as high as 1000 µg/m^3 have been reported.[68] In addition, most studies have used either inhalation or instillation as a method to deliver $PM_{2.5}$.[65] In our study, $PM_{2.5}$ was administered topically onto the ocular surface. Owing to blinking of the eyelids, the amount of particulate retained is difficult to assess and was compensated for by using the concentration selected. Nonetheless, it is worth noting that the dosage we used did not achieve levels used to induce dry eye, which is reported to occur at a dose of 5000 µg/mL.[53]

Because the MCEC in vitro work suggested that there is an increase in proinflammatory and oxidative stress molecules after $PM_{2.5}$ exposure, we used the mouse model (whose corneal epithelium is stratified) described in brief elsewhere in this article, to test the effect of $PM_{2.5}$ exposure on keratitis. We found that the particulate exposed infected eye perforated at 2 days p.i. when compared with the infected PBS exposed eyes. This finding was accompanied by an increase in viable bacterial plate count (Fig. 3E, not significant) and

Investigative Ophthalmology & Visual Science

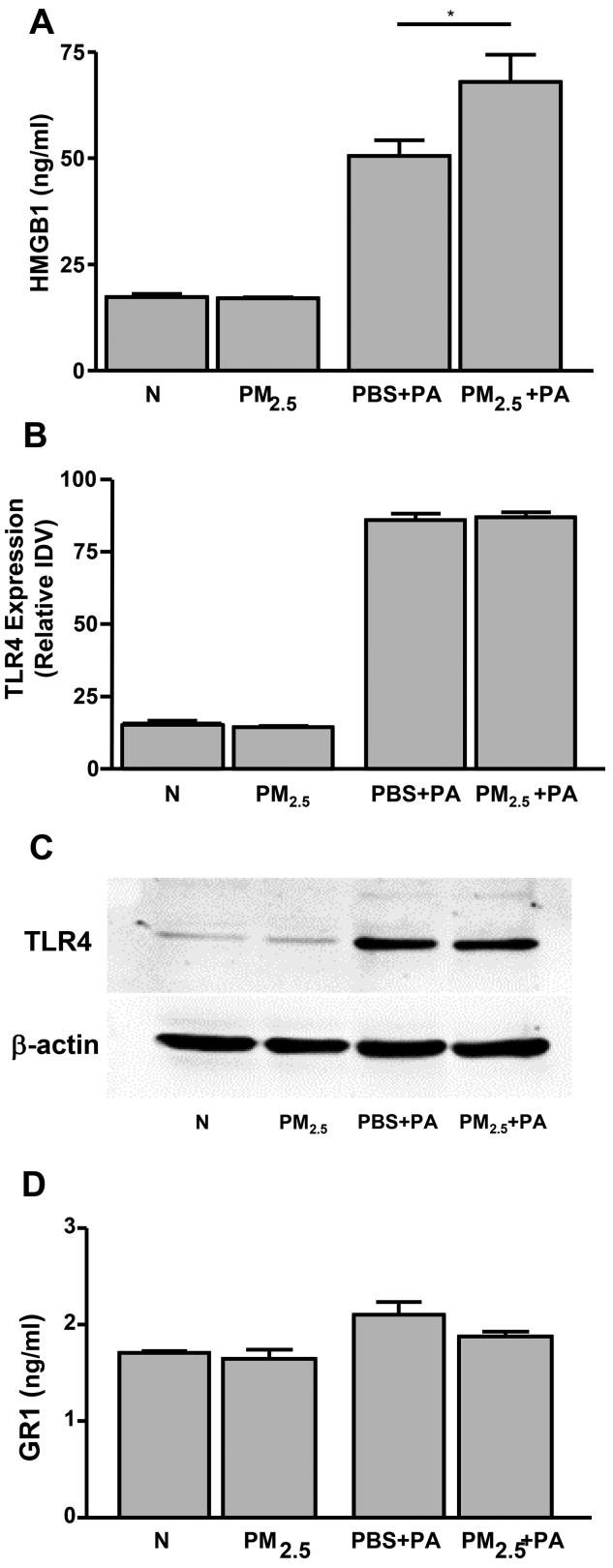

Figure 6. Protein levels of proinflammatory markers—HMGB1 (**A**) and TLR4 (**B**, **C**)—and oxidative stress marker—GR1 (**D**) in vivo. ELISA showed significantly Increased HMGB1 levels (**A**) in $PM_{2.5}$+PA versus PBS+PA. No difference was seen in uninfected normal (*N*) versus $PM_{2.5}$ exposed corneas. Western blot analysis shows increased TLR4 levels (not significantly different) in PBS+PA and $PM_{2.5}$+PA exposed groups. ELISA showed protein levels of GR1 (**D**) were unchanged across groups. Data was analyzed using the Student's *t*-test and expressed as the mean ± SEM ($n = 5$ per time). $^{*}P < 0.05$, $^{**}P < 0.01$, $^{***}P < 0.001$.

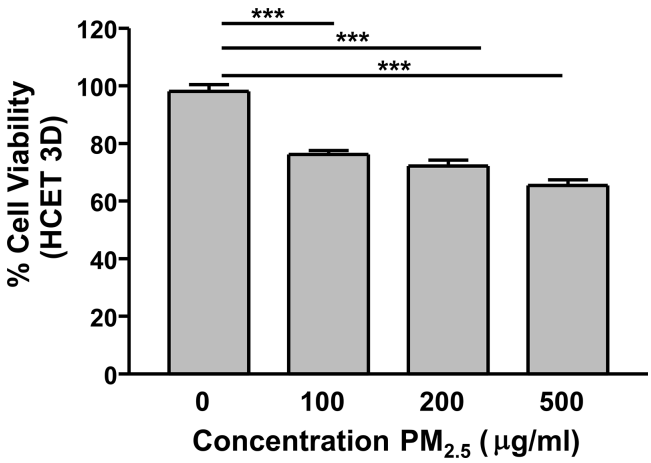

Figure 7. Effects of $PM_{2.5}$ on viability of 3D HCET cultures. Cells were exposed to 0,100, 200, and 500 μg/mL concentrations of $PM_{2.5}$ for 24 hours. Cell viability decrease was concentration dependent. Data were analyzed using one-way ANOVA followed by Bonferroni's multiple comparison test and expressed as the mean ± SEM of triplicate experiments. $^{***}P < 0.001$.

a significant increase in the number of PMN in the cornea (Fig. 3F). The evaluation of mRNA levels of proinflammatory and oxidative stress markers also showed that infected eyes exposed to $PM_{2.5}$ had increased TLR2, TLR4, IL-1β, CXCL2, HO1, GR1, GPX2, and SOD2 levels. The mRNA levels for HMGB1, an alarmin that amplifies inflammation,[69,70] decreased in all groups after exposure (Fig. 5). However, at the protein level, HMGB1, was significantly elevated (we propose through mRNA translation) only in the infected $PM_{2.5}$ compared with PBS exposed eyes. The mRNA levels of oxidative stress markers also were increased, but we did not observe any changes at the protein level for GR1 (Fig. 6D); HO1 also was tested, but protein was undetectable (data not shown) at 2 days p.i. However, oxidative stress is believed to regulate the translocation, release, and activity of HMGB1.[70] Taking this into consideration, we hypothesize that oxidative stress may be an early response to $PM_{2.5}$ exposure (after infection), which may be transient and quickly lead to HMGB1 release. This hypothesis requires further testing; however, we have clearly provided evidence that downstream activation of HMGB1 occurs after infection and $PM_{2.5}$ exposure at 2 days p.i. Future studies will be focused to determine precisely the role of ROS in release of HMGB1 and its kinetics.

Because data that are generated in a mouse system often do not translate to human applicability, we next developed a 3D culture system (that structurally mimics the stratified nature of the corneal epithelium) using immortalized HCET. After $PM_{2.5}$ exposure (Fig. 7), we found cells remained approximately 80% viable at the lower concentrations tested (e.g., 100 μg/mL) and that, at that concentration, the mRNA levels of key proinflammatory mediators HMGB1, IL-1β, and CXCL2 (Figs. 8A–C) were increased. At the highest concentration tested (500 μg/mL), only 60% of cells remained viable. These data are consistent with previous studies in primary two-dimensional HCET cultures, which also have shown that $PM_{2.5}$ treatment affected/decreased cell viability and increased levels of IL-1β.[40,41]

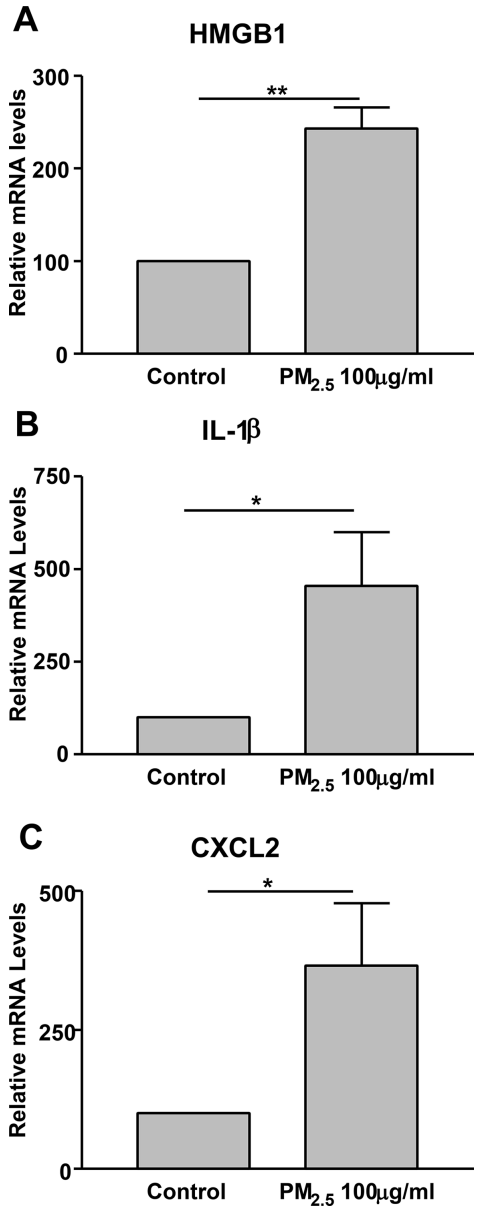

Figure 8. Effects of $PM_{2.5}$ on inflammatory molecules in 3D HCET cultures. RT-PCR shows significant change in mRNA expression for HMGB1 (**A**), IL-1β (**B**), and CXCL2 (**C**) after $PM_{2.5}$ exposure. Data were analyzed using the Student's *t*-test and expressed as the mean ± SEM of triplicate experiments. $^{*}P < 0.05$, $^{**}P < 0.01$.

In conclusion, to determine the effects of $PM_{2.5}$ on the cornea, we tested MCEC for feasibility of response to particulates, developed/modified an in vivo mouse model and tested a 3D human culture system, bridging the murine to human response. Data show that adding $PM_{2.5}$ to MCEC decreases viability and affects innate immune and oxidative stress molecules. In vivo, adding the particulate to the PA infected cornea exacerbates keratitis and leads to rapid corneal perforation.

Acknowledgments

Supported by R01EY016058 and P30EY004068 from the National Eye Institute, NIH (LDH); Research to Prevent Blindness unrestricted grant to the Department of Ophthalmology Visual and Anatomical Sciences, Kresge Eye Institute, by pilot funding from the Center for Urban Resources and Environmental Stressors (CURES), Wayne State University (LDH), and NIH Grants DK090313 and ES017829 (KZ).

Disclosure: **M. Somayajulu,** None; **S. Ekanayaka,** None; **S.A. McClellan,** None; **D. Bessert,** None; **A. Pitchaikannu,** None; **K. Zhang,** None; **L.D. Hazlett,** None

References

1. Torricelli AA, Novaes P, Matsuda M, Alves MR, Monteiro ML. Ocular surface adverse effects of ambient levels of air pollution. *Arq Bras Oftalmol*. 2011;74:377–381.
2. Rodríguez S, Querol X, Alastuey A, et al. Comparative PM10-PM2.5 source contribution study at rural, urban and industrial sites during PM episodes in Eastern Spain. *Sci Total Environ*. 2004;328:95–113.
3. O'Dell K, Ford B, Fischer EV, Pierce JR. Contribution of wildland-fire smoke to US PM2.5 and its influence on recent trends. *Environ Sci Technol*. 2019;53:1797–1804.
4. Dallmann TR, Harley RA. Evaluation of mobile source emission trends in the United States. *J Geophys Res*. 2010;115:D14305.
5. West SK, Bates MN, Lee JS, et al. Is household air pollution a risk factor for eye disease? *Int J Environ Res Public Health*. 2013;10:5378–5398.
6. Jin Q, Ma X, Wang G, Yang X, Guo F. Dynamics of major air pollutants from crop residue burning in mainland China. 2000-2014. *J Environ Sci (China)*. 2018;70:190–205.
7. Samek L. Overall human mortality and morbidity due to exposure to air pollution. *Int J Occup Med Environ Health*. 2016;29:417–426.
8. Yu G, Wang F, Hu J, Liao Y, Liu X. Value Assessment of Health Losses Caused by PM2.5 in Changsha City, China. *Int J Environ Res Public Health*. 2019;11:E2063.
9. Dockery DW, Pope CA, 3rd, Xu X, et al. An association between air pollution and mortality in six U.S. cities. *N Engl J Med*. 1993;329:1753–1759.
10. Sarkodie SA, Strezov V, Jiang Y, Evans T. Proximate determinants of particulate matter (PM2.5) emission, mortality and life expectancy in Europe, Central Asia, Australia, Canada and the US. *Sci Total Environ*. 2019;683:489–497.
11. Chen R, Yin P, Meng X, et al. Fine particulate air pollution and daily mortality. A nationwide analysis in 272 Chinese cities. *Am J Respir Crit Care Med*. 2017;196:73–81.
12. Deng X, Zhang F, Rui W, et al. PM2.5-induced oxidative stress triggers autophagy in human lung epithelial A549 cells. *Toxicol In Vitro*. 2013;27:1762–1770.
13. Xie Y, Bo L, Jiang S, et al. Individual PM2.5 exposure is associated with the impairment of cardiac autonomic modulation in general residents. *Environ Sci Pollut Res Int*. 2016;23:10255–10261.
14. Su JG, Jerrett M, Morello-Frosch R, Jesdale BM, Kyle AD. Inequalities in cumulative environmental burdens among three urbanized counties in California. *Environ Int*. 2012;40:79–87.
15. Apte K, Salvi S. Household air pollution and its effects on health. *F1000Res*. 2016;5:F1000.
16. Martenies SE, Milando CW, Williams GO, Batterman SA. Disease and health inequalities attributable to air pollutant exposure in Detroit, Michigan. *Int J Environ Res Public Health*. 2017;14:E1243.
17. Di Q, Wang Y, Zanobetti A, et al. Air pollution and mortality in the Medicare population. *N Engl J Med*. 2017;376:2513–2522.

18. Schulze F, Gao X, Virzonis D, et al. Air quality effects on human health and approaches for its assessment through microfluidic chips. *Genes (Basel)*. 2017;8:244.
19. Huang F, Pan B, Wu J, Chen E, Chen L. Relationship between exposure to PM2.5 and lung cancer incidence and mortality: a meta-analysis. *Oncotarget*. 2017;8:43322–43331.
20. Wei H, Liang F, Cheng W, et al. The mechanisms for lung cancer risk of PM2.5: induction of epithelial-mesenchymal transition and cancer stem cell properties in human non-small cell lung cancer cells. *Environ Toxicol*. 2017;32:2341–2351.
21. Raaschou-Nielsen O, Beelen R, Wang M, et al. Particulate matter air pollution components and risk for lung cancer. *Environ Int*. 2016;87:66–73.
22. Zheng Z, Zhang X, Wang J, et al. Exposure to fine airborne particulate matters induces hepatic fibrosis in murine models. *J Hepatol*. 2015;63:1397–1404.
23. Laing S, Wang G, Briazova T, et al. Airborne particulate matter selectively activates endoplasmic reticulum stress response in the lung and liver tissues. *Am J Physiol Cell Physiol*. 2010;299:C736–C749.
24. Zheng Z, Xu X, Zhang X, et al. Exposure to ambient particulate matter induces a NASH-like phenotype and impairs hepatic glucose metabolism in an animal model. *J Hepatol*. 2013;58:148–154.
25. Nam Y, Choi BH, Lee KH, et al. The role of nitric oxide in the particulate matter (PM2.5)-induced NFKB activation in lung epithelial cells. *Toxicol Lett*. 2004;148:95–102.
26. Song L, Li D, Li X, et al. Exposure to PM2.5 induces aberrant activation of NF-kappaB in human airway epithelial cells by downregulating miR-331 expression. *Environ Toxicol Pharmacol*. 2017; 50:192–199.
27. Torres-Ramos YD, Montoya-Estrada A, Guzman-Grenfell AM, et al. Urban PM2.5 induces ROS generation and RBC damage in COPD patients. *Front Biosci (Elite Ed)*. 2011;3:808–817.
28. Cohen AJ, Ross Anderson H, Ostro B, et al. The global burden of disease due to outdoor air pollution. *J Toxicol Environ Health A*. 2005;68:1301–1307.
29. Bates JT, Weber RJ, Abrams J, et al. Reactive oxygen species generation linked to sources of atmospheric particulate matter and cardiorespiratory effects. *Environ Sci Technol*. 2015;49 :13605–13612.
30. Xing YF, Xu YH, Shi MH, Lian YX. The impact of PM2.5 on the human respiratory system. *J Thorac Dis*. 2016;8:E69–E74.
31. Liu CW, Lee TL, Chen YC, et al. PM2.5-induced oxidative stress increases intercellular adhesion molecule-1 expression in lung epithelial cells through the IL-6/AKT/STAT3/NF-kappaB-dependent pathway. *Part Fibre Toxicol*. 2018;15:4.
32. Liang X, Zhang D, Liu W, et al. Reactive oxygen species trigger NF-κB-mediated NLRP3 inflammasome activation induced by zinc oxide nanoparticles in A549 cells. *Toxicol Ind Health*. 2017;33:737–745.
33. Kampfrath T, Maiseyeu A, Ying Z, et al. Chronic fine particulate matter exposure induces systemic vascular dysfunction via NADPH oxidase and TLR4 pathways. *Circ Res*. 2011;108:716–726.
34. Qiu Y, Zheng Z, Kim H, et al. Inhalation exposure to PM2.5 counteracts hepatic steatosis in mice fed high-fat diet by stimulating hepatic autophagy. *Sci Rep*. 2017;7:16286.
35. Mendez R, Zheng Z, Fan Z, et al. Exposure to fine airborne particulate matter induces macrophage infiltration, unfolded protein response, and lipid deposition in white adipose tissue. *Am J Transl Res*. 2013;5:224–234.
36. Versura P, Profazio V, Cellini M, Torreggiani A, Caramazza R. Eye discomfort and air pollution. *Ophthalmologica*. 1999;213:103–109.
37. Pokhrel AK, Bates MN, Shrestha SP, et al. Biomass stoves and lens opacity and cataract in Nepalese women. *Optom Vis Sci*. 2013;90:257–268.
38. Abou-Gareeb I, Lewallen S, Bassett K, Courtright P. Gender and blindness: a meta-analysis of population-based prevalence surveys. *Ophthalmic Epidemiol*. 2001;8:39–56.
39. Fu Q, Lyu D, Zhang L, et al. Airborne particulate matter (PM2.5) triggers autophagy in human corneal epithelial cell line. *Environ Pollut*. 2017;227:314–322.
40. Park EJ, Chae JB, Lyu J, et al. Ambient fine particulate matters induce cell death and inflammatory response by influencing mitochondria function in human corneal epithelial cells. *Environ Res*. 2017;159:595–605.
41. Yoon S, Han S, Jeon KJ, Kwon S. Effects of collected road dusts on cell viability, inflammatory response, and oxidative stress in cultured human corneal epithelial cells. *Toxicol Lett*. 2018;284:152–160.
42. Bado M, Kwende S, Shishodia S, Rosenzweig JA. Impact of dust exposure on mixed bacterial cultures and during eukaryotic cell co-culture infections. *Appl Microbiol Biotechnol*. 2017;101:7027–7039.
43. Hussey SJK, Purves J, Allcock N, et al. Air pollution alters Staphylococcus aureus and Streptococcus pneumoniae biofilms, antibiotic tolerance and colonisation. *Environ Microbiol*. 2017;19:1868–1880.
44. Miyazaki D, Fukagawa K, Fukushima A, et al. Air pollution significantly associated with severe ocular allergic inflammatory diseases. *Sci Rep*. 2019;9:18205.
45. Lee JY, Kim JW, Kim EJ, et al. Spatial analysis between particulate matter and emergency room visits for conjunctivitis and keratitis. *Ann Occup Environ Med*. 2018;30:41.
46. Hazlett L, Masinick S, Mezger B, et al. Ultrastructural, immunohistological and biochemical characterization of cultured mouse corneal epithelial cells. *Ophthalmic Res*.1996;28:50–56.
47. Peng X, Ekanayaka SA, McClellan SA, et al. Characterization of three ocular clinical isolates of P. aeruginosa: viability, biofilm formation, adherence, infectivity, and effects of glycyrrhizin. *Pathogens*. 2017;6:52.
48. Peng X, Ekanayaka SA, McClellan SA, et al. Effects of glycyrrhizin on a drug resistant isolate of Pseudomonas aeruginosa. *EC Ophthalmology*. 2018;9:265–280.
49. Ekanayaka SA, McClellan SA, Barrett RP, Kharotia S, Hazlett LD. Glycyrrhizin Reduces HMGB1 and Bacterial Load in Pseudomonas aeruginosa Keratitis. *Invest Ophthalmol Vis Sci*. 2016;57:5799–5809.
50. Ekanayaka SA, McClellan SA, Barrett RP, Hazlett LD. Topical glycyrrhizin is therapeutic for Pseudomonas aeruginosa keratitis. *J Ocul Pharmacol Ther*. 2018;34: 239–249.
51. McClellan SA, Jerome A, Suvas S, Hazlett LD. NLRC4 regulates caspase-1 and IL-1beta production in a CD11blowLy6Glow population of cells required for resistance to Pseudomonas aeruginosa keratitis. *PLoS One*. 2017;12:e0185718.
52. Zhang C, Quan Z, Wu Q, et al. Association between atmospheric particulate pollutants and mortality for cardiocerebrovascular diseases in Chinese Korean population: a case-crossover study. *Int J Environ Res Public Health*. 2018;15:2835.
53. Tan G, Li J, Yang Q, et al. Air pollutant particulate matter 2.5 induces dry eye syndrome in mice. *Sci Rep*. 2018;8:17828.
54. Camara JG, Lagunzad JK. Ocular findings in volcanic fog induced conjunctivitis. *Hawaii Med J*. 2011;70:262–265.
55. Cyrys J, Heinrich J, Hoek G, et al. Comparison between different traffic-related particle indicators: elemental carbon

(EC), PM2.5 mass, and absorbance. *J Expo Anal Environ Epidemiol*. 2003;13:134–143.

56. Xiang P, Liu RY, Sun HJ, et al. Molecular mechanisms of dust-induced toxicity in human corneal epithelial cells: water and organic extract of office and house dust. *Environ Int*. 2016;92–93:348–356.
57. Xiang P, Liu RY, Sun HJ, et al. Mechanisms of house dust-induced toxicity in primary human corneal epithelial cells: oxidative stress, proinflammatory response and mitochondrial dysfunction. *Environ Int*. 2016;89–90:30–37.
58. Liu XC, Li YJ, Wang YJ, et al. Protection of Shenlian extracts to PM2.5 infected RAW 264.7 cell damage. *Zhongguo Zhong Yao Za Zhi*. 2015;40:1977–1983.
59. Jalava PI, Hirvonen MR, Sillanpää M, et al. Associations of urban air particulate composition with inflammatory and cytotoxic responses in RAW 246.7 cell line. *Inhal Toxicol*. 2009;21:994–1006.
60. Tang Q, Huang K, Liu J, et al. Fine particulate matter from pig house induced immune response by activating TLR4/MAPK/NF-κB pathway and NLRP3 inflammasome in alveolar macrophages. *Chemosphere*. 2019;236:124373.
61. Zou W, He F, Liu S, et al. PM2.5 induced the expression of fibrogenic mediators via HMGB1-RAGE signaling in human airway epithelial cells. *Can Respir J*. 2018;2018:1817398.
62. Wu S, Wang B, Yang D, et al. Ambient particulate air pollution and circulating antioxidant enzymes: a repeated-measure study in healthy adults in Beijing, China. *Environ Pollut*. 2016;208:16–24.
63. Kwon B, Hazlett L D. Association of CD4+ T cell-dependent keratitis with genetic susceptibility to Pseudomonas aeruginosa ocular infection. *J Immunol*. 1997;159:6283–6290.
64. Hazlett LD, McClellan S, Kwon B, Barrett R. Increased severity of Pseudomonas aeruginosa corneal infection in strains of mice designated as Th1 versus Th2 responsive. *Invest Ophthalmol Vis Sci*.2000;41:805–810.
65. Wang G, Zhao J, Jiang R, Song W. Rat lung response to ozone and fine particulate matter (PM2.5) exposures. *Environ Toxicol*. 2015;30:343–356.
66. Huang T, Yu Y, Wei Y, et al. Spatial-seasonal characteristics and critical impact factors of PM2.5 concentration in the Beijing-Tianjin-Hebei urban agglomeration. *PLoS One*. 2018;13:e0201364.
67. Saraswat A, Kandlikar M, Brauer M, Srivastava A. PM2.5 population exposure in New Delhi using a probabilistic simulation framework. *Environ Sci Technol*. 2016;50:3174–3183.
68. Zhang Q, Zheng Y, Tong D, et al. Drivers of improved PM2.5 air quality in China from 2013 to 2017. *Proc Natl Acad Sci U S A*. 2019;116:24463–24469.
69. Kang R, Chen R, Zhang Q, et al. HMGB1 in health and disease. *Mol Aspects Med*. 2014;40:1–116.
70. Yu Y, Tang D, Kang R. Oxidative stress-mediated HMGB1 biology. *Front Physiol*. 2015;6:93.